PONTIFÍCIA UNIVERSIDADE CATÓLICA DO RIO GRANDE DO SUL
PRÓ-REITORIA DE PESQUISA E PÓS-GRADUAÇÃO
FACULDADE DE ODONTOLOGIA

PROGRAMA DE PÓS-GRADUAÇÃO EM ODONTOLOGIA
CIRURGIA E TRAUMATOLOGIA BUCOMAXILOFACIAL
DOUTORADO

TORQUE DE REMOÇÃO, CARACTERIZAÇÃO DE SUPERFÍCIE E HISTOMORFOMETRIA DE IMPLANTES DENTÁRIOS COM DIFERENTES SUPERFÍCIES. ESTUDO EM CÃES

TESE APRESENTADA COMO PARTE DOS REQUISITOS OBRIGATÓRIOS PARA A OBTENÇÃO DO TÍTULO DE DOUTOR EM ODONTOLOGIA NA ÁREA DE CONCENTRAÇÃO CIRURGIA E TRAUMATOLOGIA BUCOMAXILOFACIAL

LLINHA DE PESQUISA: DIAGNÓSTICO E TERAPÊUTICAS APLICADAS

Pesquisador: Charles Marin

Pesquisador Responsável: Prof. Dr. Cláiton Heitz

Porto Alegre, dezembro de 2010

SUMÁRIO

1 Lista de Abreviaturas e Símbolos:

PSHA – Plasma Spray de Hidroxiapatita

DAFI - Deposição Assistida por Feixe Iônico

DCD - Deposição Cristalina Discreta

RBMa – Resorbable Blasted Media Acid Etched

AB/AE – Alumina Blasted Acid Etched

AB/AE + RBMa - Resorbable Blasted Media Acid Etched + Alumina Blasted Acid Etched

Ti-6Al-4V - Liga de Titânio, Alumínio e Vanádio

SEM – Scanning Electron Micrography

AFM – Atomic Force Microscopy

XPS – x-ray photoelectron spectroscopy

%BIC – Bone to Implant Contact

BAFO – Bone Arial Fraction Occupied

µm – Micrometer

S_a - Surface Roughness

S_q – Square Mean Root Surface Roughness

2 Resumo

O objetivo deste estudo é determinar em cães, a influência dos tratamentos de superfície através de jateamento com biocerâmicas nos períodos iniciais de osseointegração. Quarenta e oito implantes (Ti-6Al-4V) tratados com jateamento com biocerâmica seguido de ataque ácido (RBMa), jateamento com alumina e ataque ácido (AB/AE) usado como controle, jateamento com alumina e ataque ácido com subsequente jateamento com biocerâmica e ataque ácido (AB/AE + RBMa). Três implantes de cada grupo foram destinados a caracterização físico/química por microscopia eletrônica de varredura (SEM), microscopia de força atômica (AFM) e Espectroscopia Fotoelétrica de Raios X (XPS). O estudo animal compreendeu a colocação de 48 implantes na porção proximal da tíbia (8 cães, 16 por superfície, 6 por cão) os quais permaneceram por 2 semanas in vivo. Após a eutanásia, metade dos espécimes foram destinados ao teste de torque de remoção e a outra metade foram processadas para obtençao de lâminas não descalcificadas de aproximadamente 30μm de espessura onde foram realizadas análises histomorfológica e histomorfométrica de contato osso/implante (%BIC) e fração arial de osso formado (BAFO). O teste GLM ANOVA com 95% de significância foi utilizados para análise estatística com post-hoc de Dunn. A AFM demonstrou valores de rugosidade (S_a e S_q) significante maiores do grupo AB/AE em relação aos grupos RBMa e AB/AE + RBMa. O XPS demonstrou presença de Ti, Al, O, C, N, Ca e P para os grupos RBMa e AB/AE + RBMa, os mesmos elementos foram em contrados no grupo AB/AE, juntamente com o V, exceto Ca e P. Não foram encontradas diferenças estetísticas para %COI e BAFO. Todos os grupos demonstraram bicompatibilidade com osso imaturo observado em íntimo contato com as superficies.

Palavras chave: Implantes Dentários; Materiais Biocompatíveis; Recobrimento cerâmico

3 Abstract

The aim of this study is evaluate 3 implant surfaces in dogs at early times of ossointegration. Forty eight implants (Ti-6Al4V) were used: Resorbable Blasted Media Acid Etched (RBMa), Alumina Blasted Acid Etched (AB/AE) as control group and Alumina Blasted Acid Etched + Resorbable Blasted Media Acid Etched (AB/AE + RBMa). Tree implants per group were utilized for fisico/chemical characterization (SEM, AFM and XPS). For the animal procedure 3 implants were placed on proximal tibiae bilaterally and remained for 2 weeks in vivo (8 dogs, 16 per surface, 6 per dog). Following euthanasia half of implants were torque to interface failure and other half for non-dehydrated histological processing to final sections of ≈30μm for bone to implant contact (%BIC) and bone arial fraction ocuppied (BAFO). The GLM ANOVA at 95% of significance and Dunn's post-hoc were used for statistical analysis. AB/AE group presented higher values of S_a e S_q than groups RBMa and AB/AE + RBMa. Ti, Al, O, C, N, Ca and P were observed in groups RBMa and AB/AE + RBMa, for AB/AE group Ti, Al, O, C, N and V were observed. No statistical difference was observed for histomorfometric parameters (%BIC and BAFO) among groups. All surfaces are biocompatible and osseoconductive, newly formed woven bone was observed in proximity with all surfaces.

Key words: Dental Implants; Biocompatible Materials; Ceramic Coating.

4 INTRODUÇÃO

A situação rotineiramente observada após a colocação do implante é o estabelecimento e manutenção do íntimo contato do tecido ósseo e dos implantes dentários. Esta situação tornou a implantodontia um dos tratamentos com maior índice de sucesso dentro de toda a área da saúde desde a década de 70[1]. Apesar do alto índice de sucesso, que de acordo com a literatura excede 90% após 10 anos da instalação da prótese [1-3], nos últimos anos as alterações de forma e superfície têm sido investigadas na tentativa de acelerar e/ou melhorar o processo de osseointegração em curto e longo prazo[4-7].

Alguns estudos têm demonstrado que a interação inicial entre a geometria do implante e a respectiva dimensão da frezagem realizada para a sua colocação, resulta em padrões de regeneração óssea inicial distintos, entretanto, a morfologia óssea a longo prazo também é afetada pela geometria do implante[8, 9]. Apesar dos estudos inerentes a geometria, o parâmetro mais estudado dentro da implantodontia são as alterações de superfície[4, 10-15].

Ao longo dos anos, estudos demonstraram melhoras da resposta óssea e melhora das propriedades mecânicas quando da utilização de superfícies texturizadas (rugosas), quando comparadas com as primeiras superfícies utilizadas (usinadas)[11, 16]. O processo de produção das superfícies rugosas é alcançada através de vários meios industriais, dentre elas podemos citar o ataque ácido[13, 17], anodização[18-20], jateamento com alumina[21], jateamento com sílica[5, 12], jateamento com óxido de titânio[22] ou biocerâmicas absorvíveis[23-25]. Todos estes tratamentos de superfícies geram superfícies moderadamente rugosas (média do valor absoluto de rugosidade variando em 0.5 e 2μm)[4, 15] e estão comercialmente disponíveis por mais de uma década com resultados de longo prazo aceitáveis[13, 19, 22, 26].

Enquanto o aumento da rugosidade de superfície tem melhorado a resposta inicial da osseointegração, a incorporação de cerâmicas bioativas a base de cálcio e fósforo (como o plasma spray de hidroxiapatita, PSHA) sobre a superfície dos implantes osseointegrados tem resultado em boas propriedades de osseocondução e biocompatibilidade[27-29]. Apesar das propriedades apresentadas pelas biocerâmicas, a presença de uma fraca união entre o substrato metálico e o recobrimento de PSHA, a dificuldade de uniformidade de dissolução/ absorção fizeram com que essa modalidade de recobrimento fosse descontinuada[29, 30].

Na tentativa de manter as propriedades osseocondutivas, a biocompatibilidade das biocerâmicas (a base de cálcio e fósforo) e ao mesmo tempo evitar as desvantagens inerentes dos recobrimentos PSHA, faz-se atualmente a incorporação de partículas de Ca e P em escala reduzida nas superfícies dos implantes osseointegrados. Vários são os métodos empregados para esse fim, como deposição assistida por feixe iônico (DAFI)[7, 21], sputtering[31], deposição cristalina discreta (DCD)[32, 33], jateamento com biocerâmicas absorvíveis[25], além de outros processamentos[34, 35]. A incorporação de Ca e P através do precesso de jateamento com biocerâmicas absorvíveis, a textura de superfície e a composição química de superfície (especialmente a quantidade de Ca e P) são dependentes de algumas variáveis, dentre elas destaca-se a composição do meio de jateamento, o tamanho da partícula, os parâmetros de processamento, como a pressão empregada, distância da fonte ao alvo e a presença de subseqüente tratamento por ataque ácido[10]. Devido a grande quantidade de variáveis e diferenças nos processamentos, é desconhecido o real potencial do tratamento de superfície posterior ao jateamento inicial com cerâmicas bioativas (o que diminui a presença de Ca e P disponível na superfície) no que tange a melhora da reposta óssea, nos períodos iniciais da osseintegração. Existem algumas variáveis inerentes a processo industrial para trataemnto da superfície, que levantam hipóteses tais como: Qual o real valor da limpeza seletiva? Os remanescentes de Ca e P são suficientes para melhorar a reposta óssea e qual o melhor meio absorvível para o jateamento? O objetivo deste trabalho visa elucidar estas pergutas através da caracterização de superfície, teste de torque de remoção e análise histomorfométrica em cães (anexo 1) dos seguintes tratamentos de superfície: jateamento com biocerâmica seguido de ataque ácido (RBMa), jateamento com alumina e ataque ácido (AB/AE) usado como controle, jateamento com alumina e ataque ácido com subsequente jateamento com biocerâmica e ataque ácido (AB/AE + RBMa).

5 Artigo Científico

Editorial Manager(tm) for Journal of Oral Implantology
Manuscript Draft

Manuscript Number: AAID-JOI-D-10-00156R1

Title: Histologic and Biomechanical Evaluation of Two Resorbable Blasting Media (RBM) Implant Surfaces at Early Implantation Times.

Short Title: In vivo evaluation of Two Resorbable-Blasting Media Surfaces.

Article Type: Research

Keywords: implant surface; in vivo; torque; histology; osseointegration; resorbable-blasting media

Corresponding Author: Estevam Augusto Bonfante, Ph.D

Corresponding Author's Institution: Private

First Author: Charles Marin, DDS; MS; PhD

Order of Authors: Charles Marin, DDS; MS; PhD;Estevam Augusto Bonfante, Ph.D;Ryan Jeong, PhD;Rodrigo Granato, DDS; MS; PhD;Gabriela Giro, DDS; MS; PhD;Marcelo Suzuki, DDS;Claiton Heitz, DDS; MS; PhD;Paulo G Coelho, DDS; MS; BS; MsMtE; PhD

Abstract: This study evaluated 3 implant surfaces in a dog model: Resorbable-blasting media + acid-etched (RBMa), alumina-blasting + acid-etched (AB/AE), and AB/AE + RBMa (Hybrid). All the surfaces were texturized, and Ca and P were present for the RBMa and Hybrid surfaces. Following 2 weeks in vivo no significant differences were observed for torque, bone-to-implant contact, and bone-area fraction occupied measurements. Newly formed woven bone was observed in proximity with all surfaces.

Histologic and Biomechanical Evaluation of Two Resorbable Blasting Media (RBM) Implant Surfaces at Early Implantation Times.

Charles Marin[1] PhD, Estevam A. Bonfante[2]* PhD, Ryan Jeong[3] BS, PhD, Rodrigo Granato [4] PhD, Gabriela Giro [5] PhD, Marcelo Suzuki [6] DDS, Claiton Heitz[1] PhD, Paulo G. Coelho [3] PhD

1- Department of Oral and Maxillofacial Surgery, Pontificia Universidade Católica do Rio Grande Do Sul, Porto Alegre, RS, Brazil.

2- Department of Prosthodontics, University of São Paulo – Bauru School of Dentistry, Bauru, SP, Brazil.

3- Department of Biomaterials and Biomimetics, New York University, New York, NY USA.

4- Department of Dentistry, Universidade Federal de Santa Catarina, Florianópolis, SC, Brazil

5- Department of Oral Surgery and Diagnosis, Faculdade de Odontologia de Araraquara, UNESP, Araraquara, SP, Brazil.

6- Department of Prosthodontics, Tufts University School of Dental Medicine, Boston, MA, USA

* **Corresponding author**: Estevam A. Bonfante

Short Title: In vivo evaluation of Two Resorbable-Blasting Media Surfaces.

Abstract:

This study evaluated 3 implant surfaces in a dog model: Resorbable-blasting media + acid-etched (RBMa), alumina-blasting + acid-etched (AB/AE), and AB/AE + RBMa (Hybrid). All the surfaces were texturized, and Ca and P were present for the RBMa and Hybrid surfaces. Following 2 weeks in vivo no significant differences were observed for torque, bone-to-implant contact, and bone-area fraction occupied measurements. Newly formed woven bone was observed in proximity with all surfaces.

Keywords: implant surface; *in vivo*; torque; histology; osseointegration; resorbable-blasting media

Introduction

The contact between bone and endosseous implants is usually well established and maintained after implant placement, resulting in a success rate often exceeding 90% over 10 years[36, 37]. Because of its high success, the development of endosseous implants is also one of the most studied modalities in dentistry[4]. Past investigations have shown that surface modification methods have been successful in increasing the host response to the implants, resulting in better long-term bone morphology as well as the initial interaction between the host and the implant[21]. As a result, surface modifications in surface texture and chemistry such as increasing the roughness, addition of calcium and phosphorus based bioceramic coatings have been one of the most investigated aspect of the implant studies[21, 38-40].

Over the years, surface texture modification has proven to be effective in increasing the host response in *in vivo*, *in vitro*, and *ex vivo* studies[41]. More bone-to-implant interaction has been shown in surfaces with increased roughness as compared to machined or smooth surfaces, but the best osseointegration measurable by Bone to Implant Contact (BIC) have been shown in the microscopically moderately rough surfaces (Ra between 0.5 and 2μm)[21, 38-40]. Surface roughness can be achieved in a variety of ways which include acid-etching, anodization, and grit-blasting with nonresorbable media (alumina, silica, titanium oxides,) or resorbable blasting media (RBM) such as hydroxiapatite, tricalcium phosphates, or a combination of Ca-P phases followed by acid-etching or passivation treatment that leaves little to absent amount of Ca and P on the final product[21].

Increasing the surface roughness have resulted in improved early host-to-implant response, but a surface chemistry alteration involving bioceramic coating of implants using the thick plasma-sprayed hydroxyapatite (PSHA) have shown to result in higher degrees of fixation at earlier implantation times compared to moderately rough uncoated implants[27, 29, 30]. However, PSHA-coated implants rely on mechanical interlocking between the grit-blasted or etched metallic surfaces and the ceramic-like PSHA coating, and this physical interaction among the bulk metallic, metallic oxide, and bioceramic surface has been considered a weak link based on frequent adhesive failures that have reportedly occurred on different implant configurations[27, 29, 30].

In an attempt to take advantage of increased osseoconductiveness of the Ca-P while avoiding the mechanical drawbacks of PSHA coatings, integration of Ca-P particles at a reduced amount through various techniques such as ion beam-assisted deposition[31, 42, 43], sputtering[22, 26], discrete crystalline deposition[32, 33, 44, 45], and RBM[25, 46] processes have shown promising results as compared to uncoated, roughened implants. Specific to RBM processing, various factors such as blasting media composition, blasting particle size, processing parameters such as blasting pressure and distance, and subsequent acid-etching are shown to have effect on early host-to-implant surfaces[21], but the present standing on the matter is still inconclusive on the amount and the form of Ca-P that demonstrates optimal host-bone interaction. Consequently, the aim of this investigation was to evaluate the biomechanical fixation and to histomorphologically and histomorphometrically characterize three different implant surfaces: 1) RBM + acid-etching (RBMa); 2) alumina blasting + acid-etching (AB/AE); and 3) AB/AE + RBMa surface (Hybrid).

Materials and Methods:

The endosseuous Ti-6Al-4V implants (MIS Implant Technologies Ltd., Shlomi, Israel) utilized in this study were 3.75 mm in diameter by 10mm in length. Three surface modifications investigated are RBM + acid-etching (RBMa), alumina blasting + acid-etching (AB/AE), and the AB/AE + RBMa surface (Hybrid).

The AB/AE surface was achieved by blasting the surface with large particles of Al_2O_3 with a size of ~300-400 microns followed by acid-etching with hydrochloric/sulfuric acid. The RBMa surface was achieved by blasting with HA/TCP (20/80 percent ratio) particles with a size of ~200-400 microns followed by cleaning with HNO_3 at a room temperature for 10 minutes. The hybrid surface (AB/AE+ RBMa) surface was obtained by first applying the AB/AE treatment and subsequently applying the RBMa surface treatment. All implant surfaces were sterilized under gamma radiation.

Surface Characterization

Nine implants (n=3 each group) were used for surface topography assessment by scanning electron microscopy (SEM) and atomic force microscopy (AFM). SEM (Philips XL 30, Eindhoven, The Netherlands) was performed at various magnifications under an acceleration voltage of 15kV. Surface three-dimensional (3D) imaging was collected by AFM (Nanoscope IIIa Multimode system, Digital Instruments, Santa Barbara, CA, USA) in contact mode. A scanner with a maximum 125-μm horizontal and 5-μm vertical range and a 200-μm Si_3N_4 cantilever tip using a constant force of 0.12N/m was used. The region analyzed was the flat part of the implant cutting edges, and 35 x 35 μm scan areas were used [34, 35]. Three scans per implant were performed and S_a

(arithmetic average high deviation) and S_q (root mean square) parameters determined. Statistical analysis at 95% level of significance was performed by one-way ANOVA.

Surface specific chemical assessment was performed by x-ray photoelectron spectroscopy (XPS). The implants were inserted in a vacuum transfer chamber and degassed to 10^{-7} torr. The samples were then transferred under vacuum to a Kratos Axis 165 multitechnique XPS spectrometer (Kratos Analytical Inc., Chestnut Ridge, NY, USA). Survey and high-resolution spectra were obtained using a 165 mm mean radius concentric hemispherical analyzer operated at constant pass energy of 160 eV for survey and 80 eV for high resolution scans. The take off angle was 90^o and a spot size of 150 μm x 150 μm was used. The implant surfaces were evaluated at flat part of tread in 3 different locations.

In Vivo Laboratory Model

For the animal model, 16 implants of each of the 3 surfaces were utilized. The study comprised of 8 adult male beagles dogs with ~1.5 years of age. The protocol received the approval of the Ethics Committee for Animal Research at Pontifícia Universidade Católica do Rio Grande do Sul, Porto Alegre, Brazil (Protocol number 09/00124).

Prior to general anesthesia, IM atropine sulfate (0,044 mg/kg) and xilazyne chlorate (8 mg/kg) were administered. A 15mg/Kg ketamine chlorate dose was then utilized to achieve general anesthesia.

The proximal medial tibia on right side was initially shaved with a razor blade and followed by the application of antiseptic iodine solution. An incision through the skin of

~5 cm in length was utilized for access to the periosteum, which was elevated for bone exposure.

Standardized osteotomies were made with sequential drills (pilot drill, followed by 2 mm, 2.5 mm, 3.0 mm, 3.5 mm) at 1.200 rpm under abundant saline irrigation. The first implant was inserted 2 cm below the joint capsule line at the central antero-medial position of the proximal tibiae (procedures were performed bilaterally). The other two devices were placed along the distal direction at distances of 1 cm from each other along the central region of the bone. The implants were screwed into the drilled sites with a torque wrench and remained for 2 weeks. It should be noted that due to the dimensional interplay between drilling and implant design (implant threads' 3.25 mm inner diameter and the osteotomy 3.5 mm diameter), intimate contact was achieved between bone and the implant microthreads in the cervical region and healing chambers were created at regions where larger threads were present. The order in which the implants with different surfaces were placed was alternated along the tibia with starting implant being interchanged in every tibia. Balanced surgical procedures were utilized in order to allow the comparison of the torque and histology of same number of implant surfaces, surgical site (1 through 3), and animal at 2 weeks.

In order to avoid any damage to the implant-bone interface due to removal of a callus overgrowth after limb retrieval, a cover screw was installed in each implant. Standard layered suture techniques were utilized for wound closure (4-0 vicryl- internal layers, 4-0 nylon- the skin). Post-surgical medication included antibiotics (penicillin, 20.000UI/Kg) and analgesics (ketoprophen, 1ml/5Kg) for a period of 48 hours postoperatively. The euthanasia was performed by anesthesia overdose 2 weeks after placement.

At necropsy, the limbs were retrieved by sharp dissection, the soft tissue was removed by surgical blades, and initial clinical evaluation was performed to determine implant stability. Half of the implants (specimens from the right limb) were then referred to biomechanical testing, and the other half (specimens from the left limb) were processed for histology.

For the torque testing, the tibia was adapted to an electronic torque machine equipped with a 200 Ncm torque load cell (Test Resources, Minneapolis, MN, USA). Custom machined tooling was adapted to each implant internal connection and the bone block was carefully positioned to avoid specimen misalignment during testing. The implants were torqued in the counter clockwise direction at a rate of ~0.196 radians/min, and a torque versus displacement curve was recorded for each specimen.

For histology processing, the bone blocks were kept in 10% buffered formalin solution for 24h, washed in running water for 24h, and gradually dehydrated in a series of alcohol solutions ranging from 70-100% ethanol. Following dehydration, the samples were embedded in a methacrylate-based resin (Technovit 9100, Heraeus Kulzer GmbH, Wehrheim, Germany) according to the manufacturer's instructions. The blocks were then cut into slices (~300 μm thickness) aiming the center of the implant along its long axis with a precision diamond saw (Isomet 2000, Buehler Ltd., Lake Bluff, USA), glued to acrylic plates with an acrylate-based cement, and a 24h setting time was allowed prior to grinding and polishing. The sections were then reduced to a final thickness of

~30 μm by means of a series of SiC abrasive papers (400, 600, 800, 1200 and 2400) (Buehler Ltd., Lake Bluff, IL, USA) in a grinding/polishing machine (Metaserv 3000, Buehler Ltd., Lake Bluff, USA) under water irrigation[47]. The sections were then toluidine blue stained and referred to optical microscopy evaluation.

The BIC was determined at 50X-200X magnification (Leica DM2500M, Leica Microsystems GmbH, Wetzlar, Germany) by means of computer software (Leica Application Suite, Leica Microsystems GmbH, Wetzlar, Germany). The regions of bone-to-implant contact along the implant perimeter were subtracted from the total implant perimeter, and calculations were performed to determine the BIC. The bone area fraction occupied (BAFO) between threads in trabecular bone regions was determined at 100X magnification (Leica DM2500M, Leica Microsystems GmbH, Wetzlar, Germany) by means of a computer software (Leica Application Suite, Leica Microsystems GmbH, Wetzlar, Germany). The areas occupied by bone were subtracted from the total area between threads, and calculations were performed to determine the BAFO (reported in percentage values of bone area fraction occupied)[48].

Friedman's test at 95% level of significance and Dunn's post-hoc test was used for multiple comparisons between groups for Torque, BIC, and BAFO.

Results

The implant surfaces electron micrographs and 3D atomic force microscopies are presented in Figures 1 and 2, respectively. The AB/AE presented a textured surface without the presence of embedded alumina particles (Fig. 1A) while the RBMa surface electron micrographs showed that the acid etching procedure was partially effective on removing embedded blasting media particles, revealing a textured surface (Fig. 1B). The Hybrid surface presented morphology similar to the RBMa surface (Fig. 1C). The AFM assessment showed that the AB/AE surface presented significantly higher mean S_a ($p < 0.03$) and S_q ($p < 0.04$) values compared to the RBMa (Figure 3). The Hybrid surface roughness presented intermediate values (Figure 3).

The AB/AE XPS survey analysis showed peaks of Ti, Al, V, C, and O (Table 1), while the RBMa and Hybrid surfaces presented Ti, Al, Ca, C, P, N (Table 1). High-resolution spectrum evaluation showed that for all surfaces titanium was found primarily as TiO_2 with a very low level of metallic Ti, and carbon was observed primarily as hydrocarbon (C-C, C-H) with lower levels of oxidized carbon forms. For both the RBMa and Hybrid groups, calcium and phosphate were detected in varied atomic concentrations. For the RBMa and Hybrid groups, calcium and phosphate atomic concentrations ranged from ~1 to 3.5 and ~1 to ~2.5 atomic percent, respectively.

The animal surgical procedures and follow-up demonstrated no complications regarding procedural conditions, postoperative infection, or other clinical concerns. The biomechanical testing results showed that implant surface did not have a significant effect on torque to interface fracture ($p = 0.51$) (Figure 4).

Qualitative evaluation of the toluidine blue stained thin sections showed intimate contact between cortical and trabecular bone (Figure 5) for all implant surfaces, showing that all three surfaces are biocompatible and osseoconductive. At 2 weeks, newly formed woven bone was observed in close proximity with all implant surfaces (Figure 6). The histomorphometric results demonstrated that implant surface also did not have a significant effect on BIC and BAFO ($p=0.46$ and $p=0.64$, Figures 7a and 7b, respectively).

Discussion

Over the years, the implant surface modification has evolved from as-machined, smooth surfaces to microscopically moderately roughened surfaces that have shown to enhance the bone healing after the placement of implants[4, 5, 21, 38, 41]. Subsequent surface chemistry modifications such as the incorporation of bioactive ceramics have long been the focus of investigations as a positive factor for improved early bone healing. However, considering that surface chemistry modifications typically involve changes in surface topography[49] it is still unclear whether resulting topography changes alone and/or the combination with chemical modifications leads to improved osseointegration[39].

The surface treatments investigated in this study comprised an alumina-blasted/acid-etched control, a RBMa, and a hybrid surface which combined AB/AE followed by RBMa treatment. A previous study has shown that subsequent etching RBM (RBMa) substantially reduced Ca and P amounts on the surface, yet with no differences in removal torque, BIC, and BAFO when compared to a rougher control AB/AE[46]. Another investigation has observed improved torque at two times in vivo for a RBMa compared to a overall smoother dual acid-etched used as a control [25]. Because the dual-acid etched surface in the latter study resulted in lower torque values compared to the RBMa [25], it was speculated that surface texture, rather than chemistry was likely the factor influencing improved bone response. The rationale for evaluating the different surfaces at 2 weeks in vivo in the beagle dog model was based upon our previous investigations, which have shown that high degrees of biomechanical fixation occur as early as 3 weeks in the beagle dog long bones.[6, 7, 9, 14, 15, 21, 23-25, 46, 50-52] The bone healing pattern and long term remodeling dynamics has been shown to be remarkably similar between species.[53] However, the literature is sparse concerning the quantification of healing kinetics around implants between species. Although osseointegration rates are known to be higher in animal models compared to human, its quantification is yet to be experimentally determined.

The rationale of testing the hybrid surface was to bring the surface roughness of this group to an approximate scale to the AB/AE group combined with the presence of CaP achieved with subsequent RBMa treatment. Despite the not significantly different roughness between AB/AE and the Hybrid surface, the expected synergistic effect of combined roughness and chemical bonding involving implants with CaP remnants from blasting[25], early fixation, BIC, and BAFO of all three surfaces could not be confirmed. Future studies incorporating higher amounts CaP on implant surfaces are warranted.

There have been studies showing promising results concerning reduced length scale bioactive ceramic integration on implant surfaces[6, 7, 21, 25]. However, specific to RBM surfaces, various factors such as particle size, blasting media composition, blasting pressure and distance, and the subsequent acid-etching have shown to affect the early host response to the implant[21, 25, 46], and thus currently the design rationale for the surface incorporation of Ca-P still remains to be determined[39, 54].

The general results from this study shows that all three surfaces investigated are biocompatible and osseoconductive, resulting in a similar bone healing pattern with the cortical and trabecular bone in close interaction with the implant surface[8, 48]. Woven bone formation was observed in all three surfaces after the 2 weeks allowed after the initial placement.

In agreement with the biomechanical testing results, no significant differences were found among the three surfaces in regards to BIC and BAFO measurements. Thus, within the limitations of the present study, we conclude that the availability of Ca and P on the surface did not hasten early integration of textured surfaces.

Figure Legends

Figure 1) Implant surfaces' electron micrographs of A) AB/AE surface depicting a textured surface without the presence of embedded alumina particles. B) The RBMa micrograph shows a textured surface with evidence that the acid etching procedure was partially effective on removing embedded blasting media particles, and C) The Hybrid surface presenting a similar morphology to the RBMa surface.

Figure 2) 3D atomic force microscopies of A) AB/AE, B) RBMa, and C) Hybrid surface.

Figure 3) AFM assessment measurable roughness parameters showed that the AB/AE surface presented significantly higher mean S_a ($p< 0.03$) and S_q ($p< 0.04$) values compared to the RBMa. The Hybrid surface roughness presented intermediate values. The number of asterisks denotes statistically homogeneous groups.

Figure 4) Removal torque statistics summary (mean ± 95% CI) for the different surfaces at 2 weeks.

Figure 5) Representative optical microscopy montage depicting close contact between implant surfaces and cortical and trabecular bone regions (toluidine blue staining; original magnification X 25).

Figure 6) Representative histologic section at 2 weeks for A) AB/AE, B) RBMa, and C) Hybrid surfaces. Note the close proximity of newly formed woven bone with all implant surfaces.

Figure 7) A) BIC and B) BAFO statistics summary (mean ± 95% CI) for the different surfaces. The number of asterisks denotes statistically homogeneous groups.

Figure 1

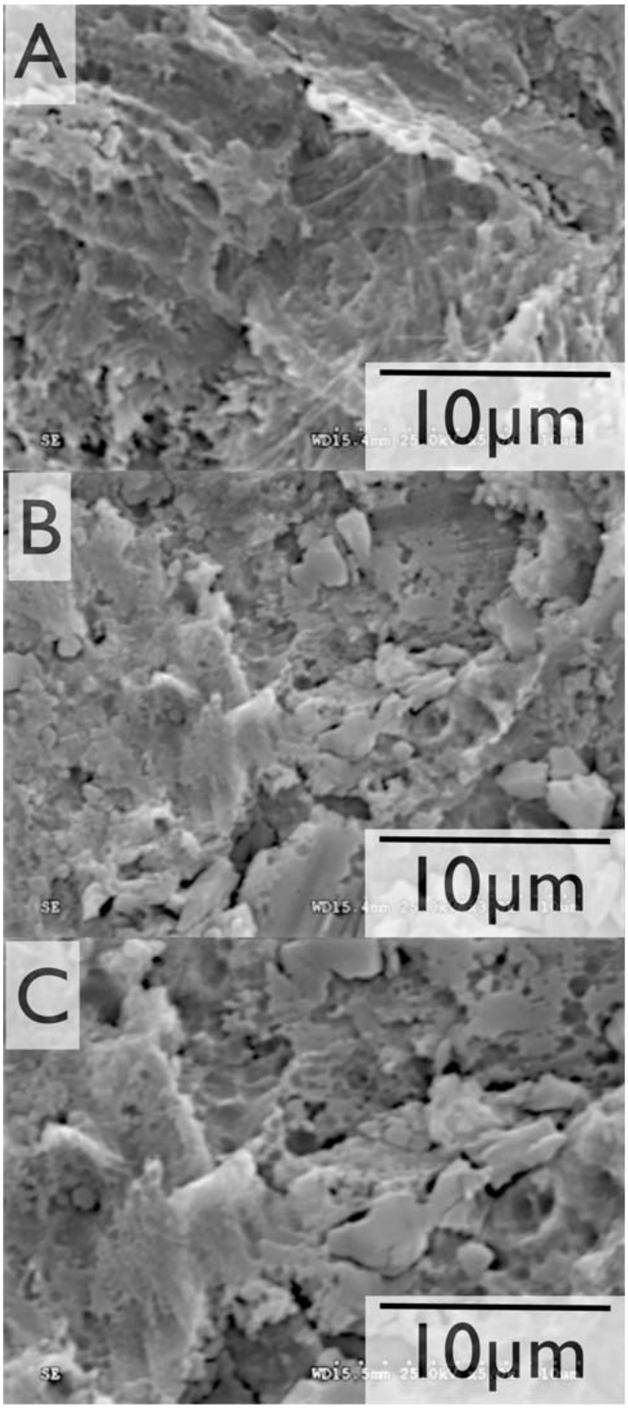

Figure 2

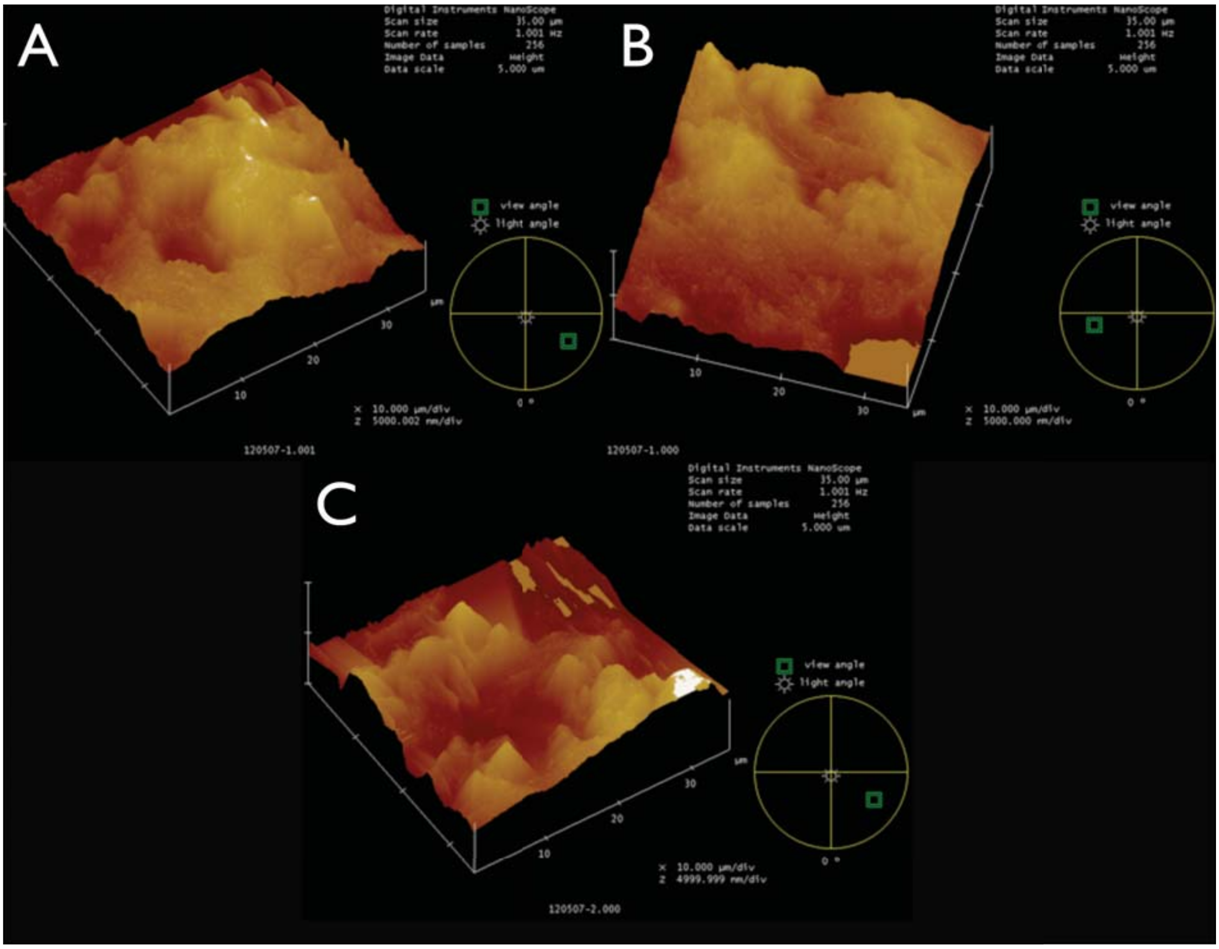
A
Digital Instruments NanoScope
Scan size 35.00 µm
Scan rate 1.001 Hz
Number of samples 256
Image Data Height
Data scale 5.000 um
view angle
light angle
X 10.000 µm/div
Z 5000.002 nm/div
120507-1.001
B
Digital Instruments NanoScope
Scan size 35.00 µm
Scan rate 1.001 Hz
Number of samples 256
Image Data Height
Data scale 5.000 um
view angle
light angle
X 10.000 µm/div
Z 5000.000 nm/div
120507-1.000
C
Digital Instruments NanoScope
Scan size 35.00 µm
Scan rate 1.001 Hz
Number of samples 256
Image Data Height
Data scale 5.000 um
view angle
light angle
X 10.000 µm/div
Z 4999.999 nm/div
120507-2.000

Figure 3

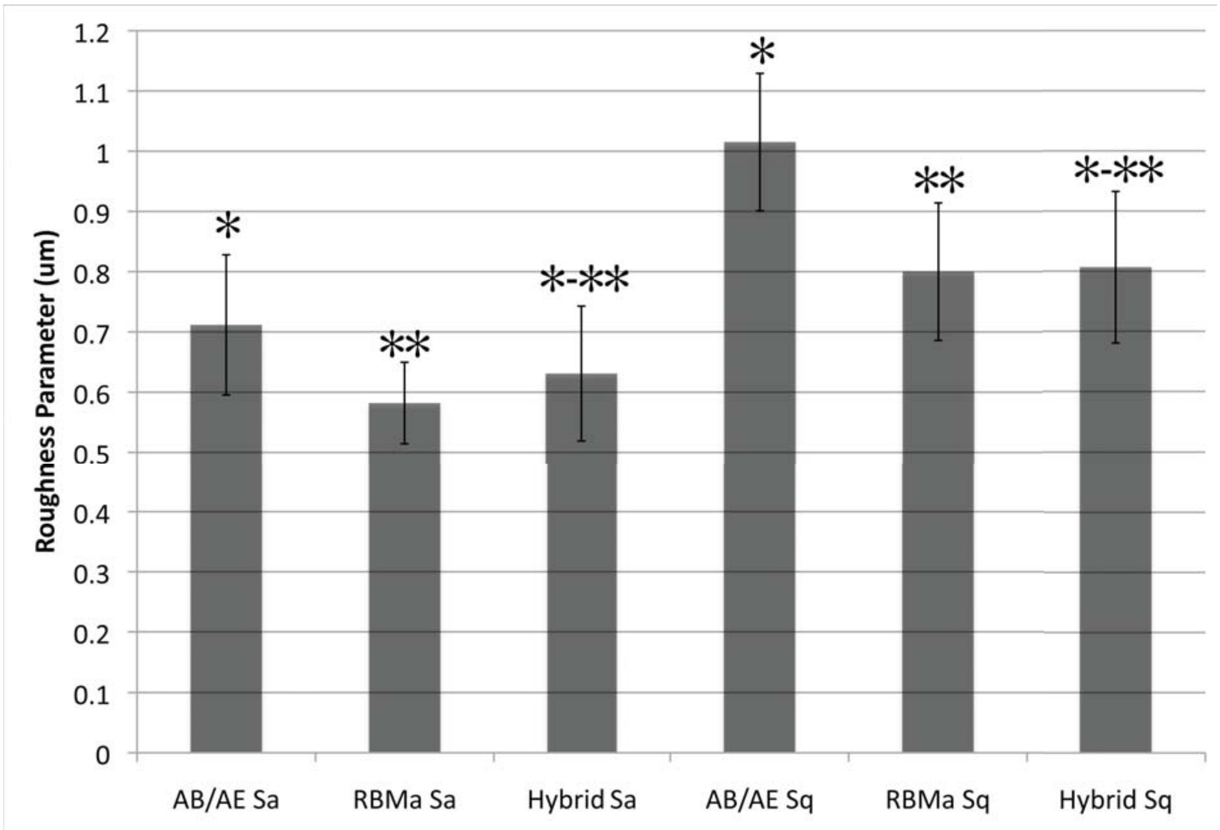

1.2
1.1
1
0.9
0.8
0.7
0.6
0.5
0.4
0.3
0.2
0.1
0
Roughness Parameter (um)
*
**
*-**
*
**
*-**
AB/AE Sa
RBMa Sa
Hybrid Sa
AB/AE Sq
RBMa Sq
Hybrid Sq

Figure 4

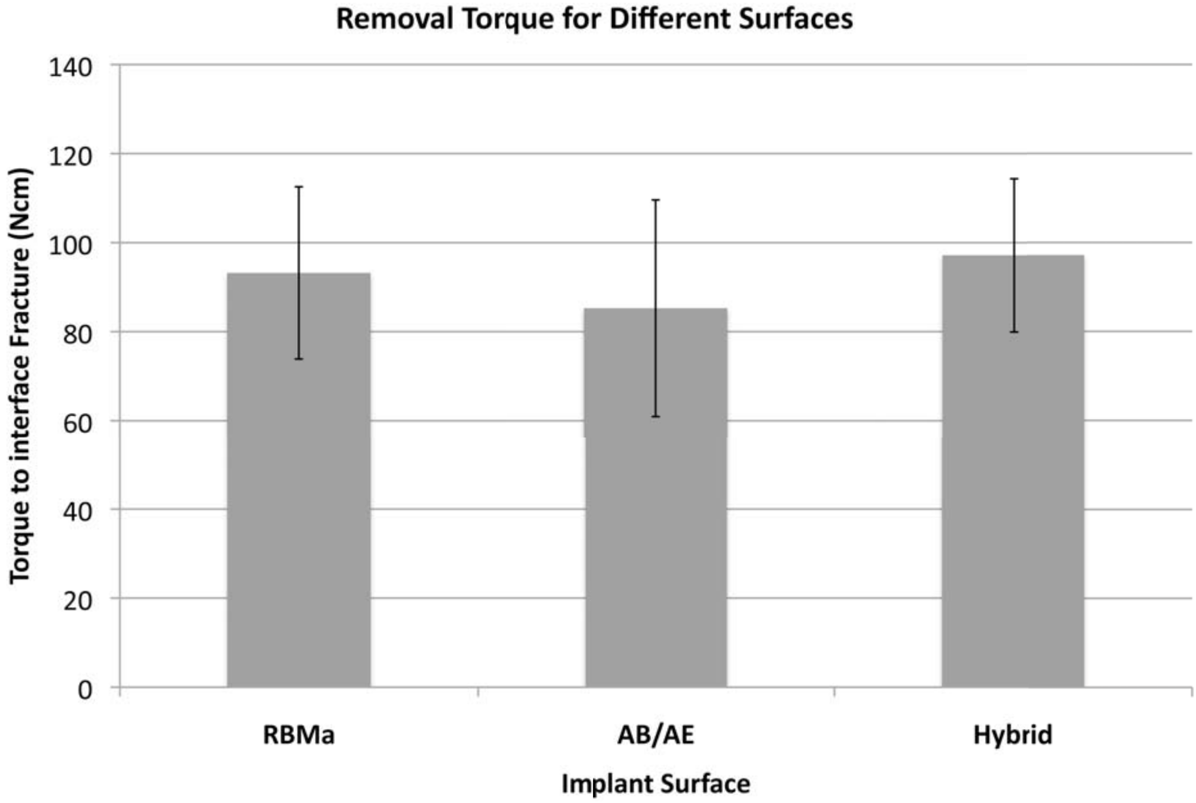
Removal Torque for Different Surfaces
140
120
100
80
60
40
20
0
Torque to interface Fracture (Ncm)
RBMa
AB/AE
Hybrid
Implant Surface

Figure 5

Figure 6

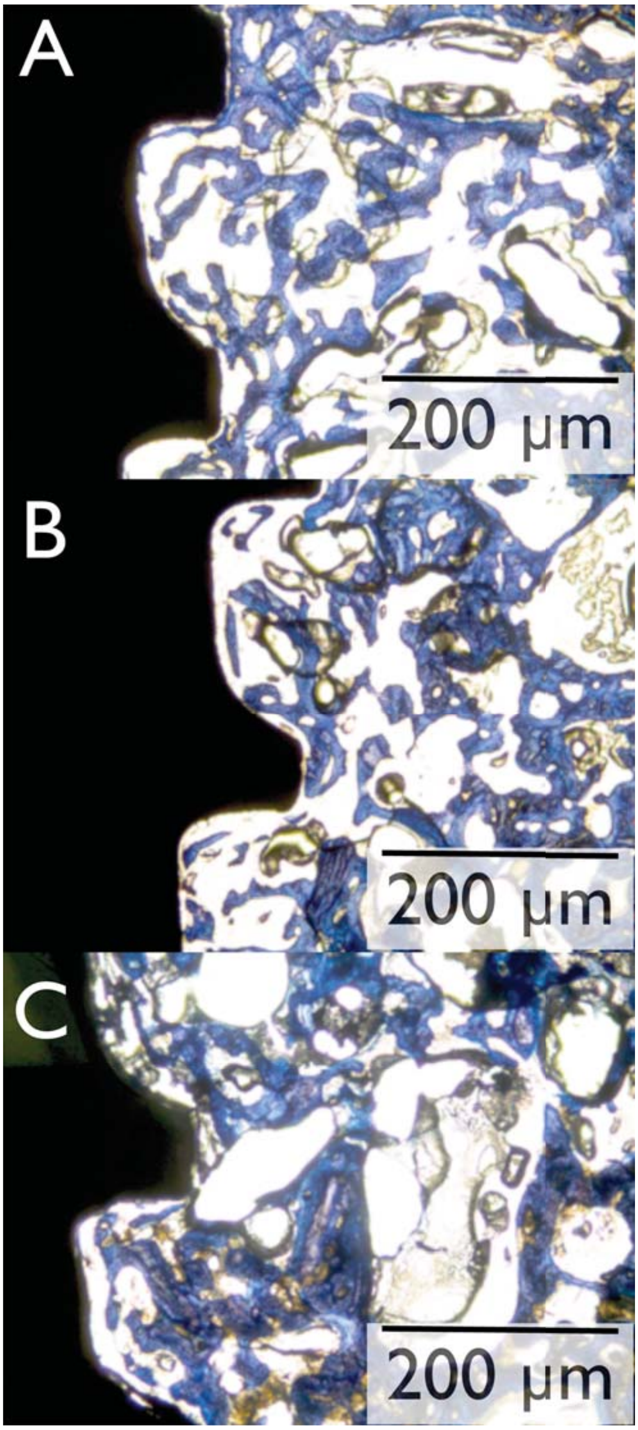

Figure 7

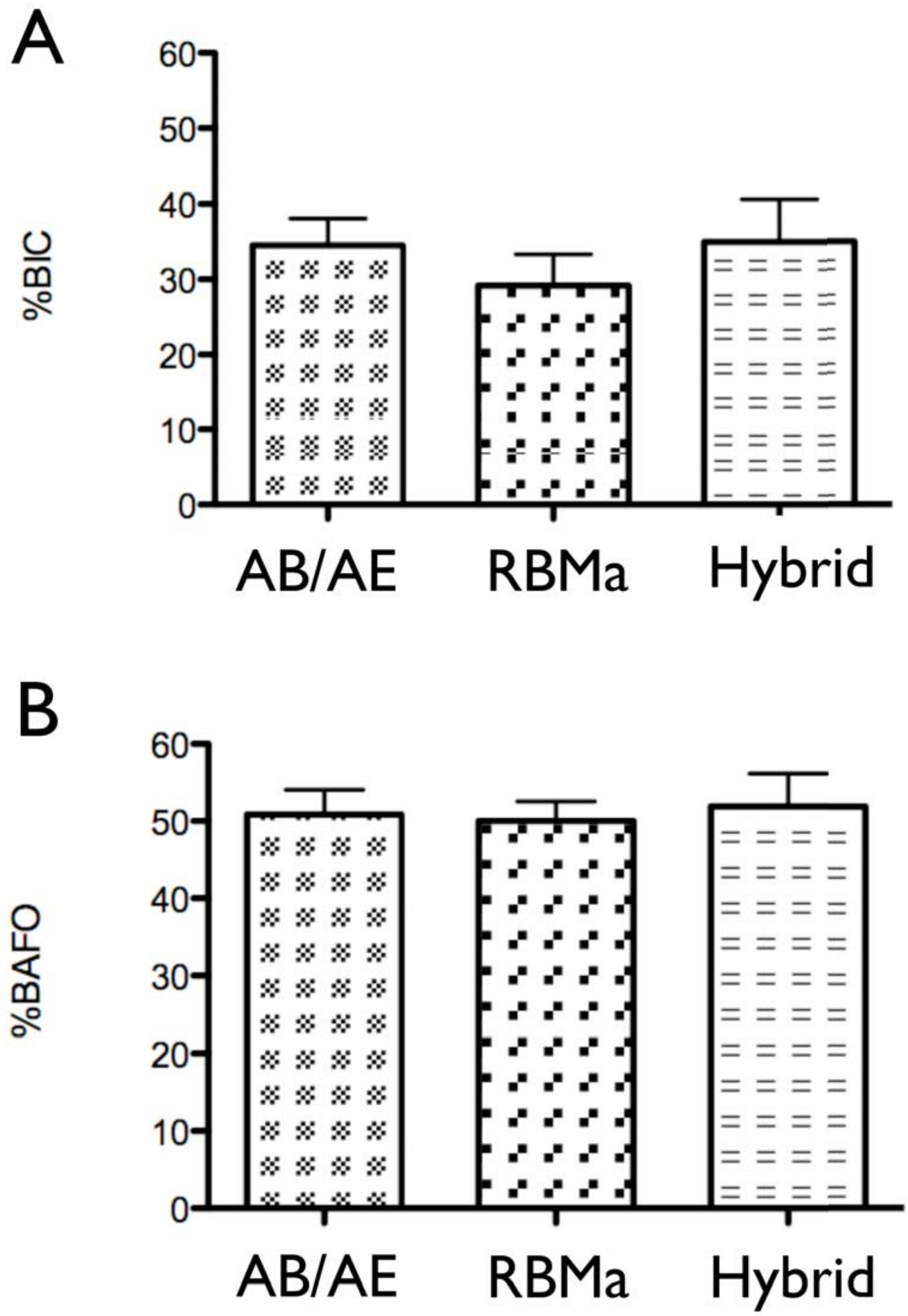
A
60
50
40
30
20
10
0
%BIC
AB/AE
RBMa
Hybrid
B
60
50
40
30
20
10
0
%BAFO
AB/AE
RBMa
Hybrid

Table 1: Average chemical composition for the three different surfaces (atomic percent).

Chemical Element (%)	AB/AE	RBMa	Hybrid
Al2p	5.73	2.61	3.06
C1s	43.1	33.07	36.89
O1s	37.89	45.59	42.4
Ti2p	10.73	13.11	14.01
V2p3	0.22	0	0
Ca2p	0	2.04	3.02
N1s	0	1.41	0.5
P2p	0	1.64	1.8

6 DISCUSSÃO GERAL

A sequência evolutiva dos implantes osseointegrados inicia com as superfícies usinadas para as superfícies atualmente consideradas superfícies rugosas, que são obtidas por uma variedade de processamentos industriais[10]. Muitos estudos têm demonstrado a melhora da resposta óssea (incluindo melhora das propriedades mecânicas) frente as superfícies moderadamente rugosas em comparação as superfícies lisas[4, 13, 16, 55]. Neste período a incorporação de recobrimentos cerâmicos bioativos têm apresentado adequado grau de biocompatibilidade e propriedades osseocondutivas (maiores que as superfícies rugosas) nos períodos iniciais da osseointegração[56-60]. Entretando, devido ao processamento industrial e das propriedades inerentes dos recobrimentos, com seus possíveis fracassos clínicos, a utilização de recobrimentos cerâmicos bioativos (inicialmente PSHA) foi drasticamente reduzido e originou novas modalidades industriais de incorporação em escala reduzida[7, 21, 25, 32].

Estudos recentes têm demostrado resultados promissores com a utilização da incorporação de cerâmicas bioativas em escala reduzida[6, 7, 25, 32, 61, 62]. Entretanto, devido as variações de forma, distribuição e propriedades químicas, pouco tem se estabelecido sobre a quantidade e forma das biocerâmicas a base de Ca e P que resultariam na melhor resposta biológica[54]. Mendes et. al.[44] demonstraram uma excelente resposta biológica para a deposição cristalina discreta de hidroxiapatita sobre uma superfície previamente tratada com duplo ataque ácido. Considerando as deposições para recobrimentos em escala nanométrica, vários trabalhos apontam alta fixação biomecânica nos períodos iniciais da osseointegração[6, 7] e altas taxas de contato osso/implante (%BIC)[61, 62]. A incorporação de Ca e P na camada de TiO_2 obtida através de jateamento com partículas de biocerâmica absorvível por vários processamentos industriais resultam na melhora do processo de osseointegração quando comparadas a implantes com tratamento de duplo ataque ácido, tanto em modelos animais[25] quanto em humanos[63]. Apesar do aumento significante de trabalhos científicos, não há uma definição do processo ideal de incorporação, no que tange a forma e a quantidade de Ca e P para as superfícies de implantes osseointegrados[54], o presente trabalho não foi capaz de definir tal método, pois de acordo com os resultados apresentados os tratamentos adicionais a superfície dos implantes mostraram-se ineficazes para a melhora do desempenho dos implantes frente as ferramentas de análise utilizadas. Apesar do %BIC ser uma das ferramentas de análise mais utilizadas para mensurar o desempenho das novas superficies, esta parece não refletir diferenças das propriedades ósseas, alguns autores relatam diferente níveis de fixacão biomecânica para mesmos valores de %BIC[24, 25]. A fração arial de osso preenchida (BAFO), já utilizada por alguns autores[48, 64] vem acrescentar uma nova forma de avaliação na área dos implantes osseointegrados porém, no presente estudo também não apontou diferenças entre os grupos.

Do ponto de vista micrométrico a rugosidade das superfícies utilizadas neste estudo podem ser consideradas moderadamente rugosas como a maioria das superfícies comercialmente disponíveis atualmente[4, 5]. Entretanto do ponto de vista científico, as superfícies apresentadas neste estudo são consideradas rugosas e não podem ser incluídas nas superfícies texturizadas em nível nanométrico estudas através de interferometria como método de AFM[35, 61, 65]. Esta questão poderia ser aprofundada por estudos adicionais das diferentes rugosidades de superfície pelos diferentes métodos de obtenção em diferentes regiões do implante[35, 61, 65], a variação na química nas diferentes areas da superfície do implante e a falta de diferença entre elas para os parâmetros analisados in vivo, não permitiriam obter uma estrutura de rugosidade apropriada.

Uma visão geral dos resultados histológicos demonstrou que todas as superfícies testadas foram biocompatíveis e osseocondutivas, apresentando o tecido ósseo em íntimo contato com a superfície do implante, tanto na região cortical quanto na região medular. Para os parâmetros histomorfométricos, não foram encontradas diferenças significativas nos parâmetros mensuráveis de osseointegração, tanto para o %BIC, BAFO quanto para o torque de remoção (TR). Bons níveis de %BIC e BAFO em 2 semanas foram observados e estão em concordância com estudos prévios, que utilizaram superfícies com incorporação de Ca e P[7, 25]. As diferenças para o torque de remoção não foram estatisticamente significantes entre todos os grupos.

Novas ferramentas de análise estão surgindo, que podem determinar propriedades mecânicas do osso formado em justaposição a superfície do implante[13] possivelmente podem ser mais sensíveis na deteção de tais diferenças e determinar as reais melhoras nos tratamentos de superfície. Mudanças na forma do macrodesenho do implante apresentam influência marcante na osseintegração[64], sendo talvez um campo pouco explorado com reais potenciais de acrescentar algo mais no campo dos implantes osseointegrados.

7 - Referências

1. Branemark PI, Hansson BO, Adell R, Breine U, Lindstrom J, Hallen O, et al. Osseointegrated implants in the treatment of the edentulous jaw. Experience from a 10-year period. Scand J Plast Reconstr Surg Suppl 1977;16:1-132.
2. Albrektsson T, Sennerby L. State of the art in oral implants. J Clin Periodontol 1991;18(6):474-81.
3. Schnitman PA, Wohrle PS, Rubenstein JE, DaSilva JD, Wang NH. Ten-year results for Branemark implants immediately loaded with fixed prostheses at implant placement. Int J Oral Maxillofac Implants 1997;12(4):495-503.
4. Albrektsson T, Wennerberg A. Oral implant surfaces: Part 1--review focusing on topographic and chemical properties of different surfaces and in vivo responses to them. Int J Prosthodont 2004;17(5):536-43.
5. Albrektsson T, Wennerberg A. Oral implant surfaces: Part 2--review focusing on clinical knowledge of different surfaces. Int J Prosthodont 2004;17(5):544-64.
6. Coelho PG, Cardaropoli G, Suzuki M, Lemons JE. Early healing of nanothickness bioceramic coatings on dental implants. An experimental study in dogs. J Biomed Mater Res B Appl Biomater 2009;88(2):387-93.
7. Granato R, Marin C, Suzuki M, Gil JN, Janal MN, Coelho PG. Biomechanical and histomorphometric evaluation of a thin ion beam bioceramic deposition on plateau root form implants: an experimental study in dogs. J Biomed Mater Res B Appl Biomater 2009;90(1):396-403.
8. Berglundh T, Abrahamsson I, Lang NP, Lindhe J. De novo alveolar bone formation adjacent to endosseous implants. Clin Oral Implants Res 2003;14(3):251-62.

9. Coelho PG, Suzuki M, Guimaraes MV, Marin C, Granato R, Gil JN, et al. Early bone healing around different implant bulk designs and surgical techniques: A study in dogs. Clin Implant Dent Relat Res 2010;12(3):202-8.
10. Coelho PG, Granjeiro JM, Romanos GE, Suzuki M, Silva NR, Cardaropoli G, et al. Basic research methods and current trends of dental implant surfaces. J Biomed Mater Res B Appl Biomater 2009;88(2):579-96.
11. Abrahamsson I, Berglundh T, Linder E, Lang NP, Lindhe J. Early bone formation adjacent to rough and turned endosseous implant surfaces. An experimental study in the dog. Clin Oral Implants Res 2004;15(4):381-92.
12. Buser D, Broggini N, Wieland M, Schenk RK, Denzer AJ, Cochran DL, et al. Enhanced bone apposition to a chemically modified SLA titanium surface. J Dent Res 2004;83(7):529-33.
13. Butz F, Aita H, Wang CJ, Ogawa T. Harder and stiffer bone osseointegrated to roughened titanium. J Dent Res 2006;85(6):560-5.
14. Coelho PG, Bonfante EA, Pessoa RS, Marin C, Granato R, Giro G, et al. Characterization of 5 Different Implant Surfaces and Their Effect on Osseointegration: A Study in Dogs. J Periodontol 2010.
15. Coelho PG, Cardaropoli G, Suzuki M, Lemons JE. Histomorphometric evaluation of a nanothickness bioceramic deposition on endosseous implants: a study in dogs. Clin Implant Dent Relat Res 2009;11(4):292-302.
16. Grizon F, Aguado E, Hure G, Basle MF, Chappard D. Enhanced bone integration of implants with increased surface roughness: a long term study in the sheep. J Dent 2002;30(5-6):195-203.
17. Klokkevold PR, Nishimura RD, Adachi M, Caputo A. Osseointegration enhanced by chemical etching of the titanium surface. A torque removal study in the rabbit. Clin Oral Implants Res 1997;8(6):442-7.

18. Huang YH, Xiropaidis AV, Sorensen RG, Albandar JM, Hall J, Wikesjo UM. Bone formation at titanium porous oxide (TiUnite) oral implants in type IV bone. Clin Oral Implants Res 2005;16(1):105-11.
19. Jungner M, Lundqvist P, Lundgren S. Oxidized titanium implants (Nobel Biocare TiUnite) compared with turned titanium implants (Nobel Biocare mark III) with respect to implant failure in a group of consecutive patients treated with early functional loading and two-stage protocol. Clin Oral Implants Res 2005;16(3):308-12.
20. Xiropaidis AV, Qahash M, Lim WH, Shanaman RH, Rohrer MD, Wikesjo UM, et al. Bone-implant contact at calcium phosphate-coated and porous titanium oxide (TiUnite)-modified oral implants. Clin Oral Implants Res 2005;16(5):532-9.
21. Suzuki M, Guimaraes MV, Marin C, Granato R, Gil JN, Coelho PG. Histomorphometric evaluation of alumina-blasted/acid-etched and thin ion beam-deposited bioceramic surfaces: an experimental study in dogs. J Oral Maxillofac Surg 2009;67(3):602-7.
22. Vercaigne S, Wolke JG, Naert I, Jansen JA. A mechanical evaluation of TiO2-gritblasted and Ca-P magnetron sputter coated implants placed into the trabecular bone of the goat: Part 1. Clin Oral Implants Res 2000;11(4):305-13.
23. Coelho PG, Lemons JE. Physico/chemical characterization and in vivo evaluation of nanothickness bioceramic depositions on alumina-blasted/acid-etched Ti-6Al-4V implant surfaces. J Biomed Mater Res A 2009;90(2):351-61.
24. Granato R, Marin C, Gil JN, Chuang SK, Dodson TB, Suzuki M, et al. Thin Bioactive Ceramic-Coated Alumina-Blasted/Acid-Etched Implant Surface Enhances Biomechanical Fixation of Implants: An Experimental Study in Dogs. Clin Implant Dent Relat Res 2009.
25. Marin C, Granato R, Suzuki M, Gil JN, Piattelli A, Coelho PG. Removal Torque and Histomorphometric Evaluation of Bioceramic Grit-Blasted/Acid-Etched and Dual Acid-

Etched Implant Surfaces: An Experimental Study in Dogs. J Periodontol 2008;79(10):1942-49.

26. Vercaigne S, Wolke JG, Naert I, Jansen JA. A histological evaluation of TiO2-gritblasted and Ca-P magnetron sputter coated implants placed into the trabecular bone of the goat: Part 2. Clin Oral Implants Res 2000;11(4):314-24.

27. Kay J. Calcium Phosphate Coatings for Dental Implants. Dental Clinics of North America 1992;36:1-18.

28. Kim H, Camata RP, Vohra YK, Lacefield WR. Control of phase composition in hydroxyapatite/tetracalcium phosphate biphasic thin coatings for biomedical applications. J Mater Sci Mater Med 2005;16(10):961-6.

29. Lacefield WR. Hydroxyapatite coatings. Ann N Y Acad Sci 1988;523:72-80.

30. Lacefield WR. Current status of ceramic coatings for dental implants. Implant Dent 1998;7(4):315-22.

31. Yang Y, Kim KH, Ong JL. A review on calcium phosphate coatings produced using a sputtering process--an alternative to plasma spraying. Biomaterials 2005;26(3):327-37.

32. Davies JE. Bone bonding at natural and biomaterial surfaces. Biomaterials 2007;28(34):5058-67.

33. Mendes VC, Moineddin R, Davies JE. Discrete calcium phosphate nanocrystalline deposition enhances osteoconduction on titanium-based implant surfaces. J Biomed Mater Res A 2009;90(2):577-85.

34. Meirelles L, Albrektsson T, Kjellin P, Arvidsson A, Franke-Stenport V, Andersson M, et al. Bone reaction to nano hydroxyapatite modified titanium implants placed in a gap-healing model. J Biomed Mater Res A 2008;87(3):624-31.

35. Meirelles L, Arvidsson A, Andersson M, Kjellin P, Albrektsson T, Wennerberg A. Nano hydroxyapatite structures influence early bone formation. J Biomed Mater Res A 2008;87(2):299-307.

36. Chuang SK, Tian L, Wei LJ, Dodson TB. Predicting dental implant survival by use of the marginal approach of the semi-parametric survival methods for clustered observations. J Dent Res 2002;81(12):851-5.

37. Chuang SK, Wei LJ, Douglass CW, Dodson TB. Risk factors for dental implant failure: a strategy for the analysis of clustered failure-time observations. J Dent Res 2002;81(8):572-7.

38. Wennerberg A, Albrektsson T. Effects of titanium surface topography on bone integration: a systematic review. Clin Oral Implants Res 2009;20 Suppl 4:172-84.

39. Wennerberg A, Albrektsson T. Structural influence from calcium phosphate coatings and its possible effect on enhanced bone integration. Acta Odontol Scand 2009:1-8.

40. Wennerberg A, Albrektsson T. On implant surfaces: a review of current knowledge and opinions. Int J Oral Maxillofac Implants 2010;25(1):63-74.

41. Elias CN, Meirelles L. Improving osseointegration of dental implants. Expert Rev Med Devices 2010;7(2):241-56.

42. Coelho P.G., Lemons J.E. IBAD Nanothick Bioceramic Incorporation on Metallic Implants for Bone Healing Enhancement. From Physico/Chemical Characterization to In-vivo Performance Evaluation. . Paper presented at: Nanotech 2005, 2005; Anaheim, CA.

43. Park YS, Yi KY, Lee IS, Han CH, Jung YC. The effects of ion beam-assisted deposition of hydroxyapatite on the grit-blasted surface of endosseous implants in rabbit tibiae. Int J Oral Maxillofac Implants 2005;20(1):31-8.

44. Mendes VC, Moineddin R, Davies JE. The effect of discrete calcium phosphate nanocrystals on bone-bonding to titanium surfaces. Biomaterials 2007;28(32):4748-55.

45. Orsini G, Piattelli M, Scarano A, Petrone G, Kenealy J, Piattelli A, et al. Randomized, controlled histologic and histomorphometric evaluation of implants with nanometer-scale calcium phosphate added to the dual acid-etched surface in the human posterior maxilla. J Periodontol 2007;78(2):209-18.

46. Marin C, Granato R, Suzuki M, Janal MN, Gil JN, Nemcovsky C, et al. Biomechanical and histomorphometric analysis of etched and non-etched resorbable blasting media processed implant surfaces: an experimental study in dogs. J Mech Behav Biomed Mater 2010;3(5):382-91.

47. Donath K, Breuner G. A method for the study of undecalcified bones and teeth with attached soft tissues. The Sage-Schliff (sawing and grinding) technique. J Oral Pathol 1982;11(4):318-26.

48. Leonard G, Coelho P, Polyzois I, Stassen L, Claffey N. A study of the bone healing kinetics of plateau versus screw root design titanium dental implants. Clin Oral Implants Res 2009;20(3):232-9.

49. Dohan Ehrenfest DM, Coelho PG, Kang BS, Sul YT, Albrektsson T. Classification of osseointegrated implant surfaces: materials, chemistry and topography. Trends Biotechnol 2010;28(4):198-206.

50. Suzuki M, Guimaraes MV, Marin C, Granato R, Fernandes CA, Gil JN, et al. Histomorphologic and bone-to-implant contact evaluation of dual acid-etched and bioceramic grit-blasted implant surfaces: an experimental study in dogs. J Oral Maxillofac Surg 2010;68(8):1877-83.

51. Suzuki M, Calasans-Maia MD, Marin C, Granato R, Gil JN, Granjeiro JM, et al. Effect of surface modifications on early bone healing around plateau root form implants: an experimental study in rabbits. J Oral Maxillofac Surg 2010;68(7):1631-8.

52. Coelho PG, Granato R, Marin C, Bonfante EA, Janal MN, Suzuki M. Biomechanical and bone histomorphologic evaluation of four surfaces on plateau root form implants: an experimental study in dogs. Oral Surg Oral Med Oral Pathol Oral Radiol Endod 2010;109(5):e39-45.

53. Garetto LP, Chen J, Parr JA, Roberts WE. Remodeling dynamics of bone supporting rigidly fixed titanium implants: a histomorphometric comparison in four species including humans. Implant Dent 1995;4(4):235-43.

54. Lemons JE. Biomaterials, biomechanics, tissue healing, and immediate-function dental implants. J Oral Implantol 2004;30(5):318-24.

55. Wennerberg A, Ektessabi A, Albrektsson T, Johansson C, Andersson B. A 1-year follow-up of implants of differing surface roughness placed in rabbit bone. Int J Oral Maxillofac Implants 1997;12(4):486-94.

56. Cheang P, Khor KA. Addressing processing problems associated with plasma spraying of hydroxyapatite coatings. Biomaterials 1996;17(5):537-44.

57. de Bruijn JD, Bovell YP, van Blitterswijk CA. Structural arrangements at the interface between plasma sprayed calcium phosphates and bone. Biomaterials 1994;15(7):543-50.

58. deGroot K KC, Wolke JGC, deBieck-Hogervorst JM,. Plasma-sprayed coating of calcium phosphate. In: Yamamuro T HL, Wilson J editor. Handbook of Bioactive ceramics, vol II, Calcium phosphate and Hydroxyapatite ceramics. Boca Raton: CRC Press; 1990. p. 17-25.

59. Ong JL, Carnes DL, Bessho K. Evaluation of titanium plasma-sprayed and plasma-sprayed hydroxyapatite implants in vivo. Biomaterials 2004;25(19):4601-6.

60. Yang CY, Wang BC, Lee TM, Chang E, Chang GL. Intramedullary implant of plasma-sprayed hydroxyapatite coating: an interface study. J Biomed Mater Res 1997;36(1):39-48.

61. Meirelles L, Currie F, Jacobsson M, Albrektsson T, Wennerberg A. The effect of chemical and nanotopographical modifications on the early stages of osseointegration. Int J Oral Maxillofac Implants 2008;23(4):641-7.

62. Meirelles L, Melin L, Peltola T, Kjellin P, Kangasniemi I, Currie F, et al. Effect of hydroxyapatite and titania nanostructures on early in vivo bone response. Clin Implant Dent Relat Res 2008;10(4):245-54.
63. Shibli JA, Grassi S, Piattelli A, Pecora GE, Ferrari DS, Onuma T, et al. Histomorphometric evaluation of bioceramic molecular impregnated and dual acid-etched implant surfaces in the human posterior maxilla. Clin Implant Dent Relat Res 2010;12(4):281-8.
64. Marin C, Granato R, Suzuki M, Gil JN, Janal MN, Coelho PG. Histomorphologic and histomorphometric evaluation of various endosseous implant healing chamber configurations at early implantation times: a study in dogs. Clin Oral Implants Res 2010;21(6):577-83.
65. Meirelles L, Arvidsson A, Albrektsson T, Wennerberg A. Increased bone formation to unstable nano rough titanium implants. Clin Oral Implants Res 2007;18(3):326-32.

8 ANEXO 1

Pontifícia Universidade Católica do Rio Grande do Sul
PRÓ-REITORIA DE PESQUISA E PÓS-GRADUAÇÃO
COMITÊ DE ÉTICA PARA O USO DE ANIMAIS

Ofício 021/10 – CEUA

Porto Alegre, 11 de março de 2010.

Senhor Pesquisador:

O Comitê de Ética para o Uso de Animais apreciou e aprovou seu protocolo de pesquisa, registro CEUA 09/00124, intitulado: **"Torque de remoção, caracterização de superfície e contato osso/implante de implantes dentários com diferentes superfícies. Estudo em cães".**

Sua investigação está autorizada a partir da presente data.

Atenciosamente,

Profa. Dra. Anamaria Gonçalves Feijó
Coordenadora do CEUA – PUCRS

Ilmo. Sr.
Prof. Dr. Claiton Heitz
N/Universidade

PUCRS

Campus Central
Av. Ipiranga, 6690 – Prédio 60, sala 314
CEP: 90610-000
Fone/Fax: (51) 3320-3345
E-mail: ceua@pucrs.br